

FIELD INDUCED SHAPE MODIFICATION FOR THE ZrO/W(100) SCHOTTKY CATHODE

K. Liu, G.A. Schwind, L.W. Swanson

FEI Co. Hillsboro, OR 97124

The frequently observed current density drift after a change in the extractor voltage for the ZrO/W(100) Schottky cathode has been investigated. It has been found that a reversible, field dependant change in the equilibrium shape of the cathode end-form occurs that results in three distinct shapes noted in the Fig. 1 top down SEM photos. Although these shapes have been observed previously^{1,2,3}, the purpose of this study is to elucidate the conditions under which they occur. The more rounded stage 0 end-form occurs for all emitter radii investigated in this study (i.e., 200 to 900 nm) when the angular current density $I' \leq 0.25$ mA/sr. The intermediate stage 1 and the more stable stage 2 end-forms occur for $I' \geq 0.5$ mA/sr. The duration of the progression from stage 0 to 2 is typically in excess of 100 hours at $T = 1800$ K and an I' range of 0.25 to 1.0 mA/sr. Since these transitions involve movement of substantial material via surface diffusion, significant temperature dependence for the transition times is expected

These shape changes result from the well known competition between the thermodynamic surface tension and electric field stress forces⁴. The dominance of the surface tension force results in the more rounded stage 0 end-form whereas the dominance of the field stress force results in the growth of the low surface free energy (100), (110) and (112) planes as seen in the stage 1 and 2 end-forms of Fig 1. Competition between of the expanding (011) and (112) facets which intersect the central (100) facet determines the occurrence of the stage 1 or 2 end-forms. Ultimately, the (110) facet growth dominates and leads to the stage 2 truncated pyramidal shaped end-form with four (110) side facets. The intersections between the latter planes lead to sharp ridges and local field enhancement. Fortunately, the current density distribution is not affected by this local field enhancement since the well-known selective work function lowering of the (100) plane overshadows the local field enhancement and leads to selective emission from the central (100) plane¹.

A time-dependant variation of the field dependant current density $J(F)$ is caused by a change in the local field factor β (where $\beta = F/V$) due to the Fig. 1 shape modifications. For micro probe applications of this source, the latter has the undesirable effect of causing a time dependant variation in the current emanating from a small solid angle of emission centered on the (100) plane at constant applied voltage V . Table I summarizes the measured variation in flat size and β for the various stages of a particular source at the indicated operating parameters. Since $J(F) \propto \exp[(\beta V)^{1/2} / kT]$ the variations in β noted in Table I for the various stages will lead to a time dependent change in $J(F)$ if a stage transition is triggered. Fortunately, these shape changes at $T = 1800$ K are such that the significant drift in $J(F)$ during a stage transition is less than 100 hrs.

Finally, it has been observed¹ that for the stage 0 end-form and $I' \leq 0.2$ mA/sr another form of current instability occurs when the rounded central (100) net planes successively shrink in size as the terrace atoms migrate toward the emitter shank. This net plane collapse leads to a repetitive perturbation in the current from the central portion of the (100) flat that can last several hours. This instability is not

observed for operating conditions such that stage 1 or 2 end-forms are maintained, i.e. $I' > 0.25$ mA/sr.

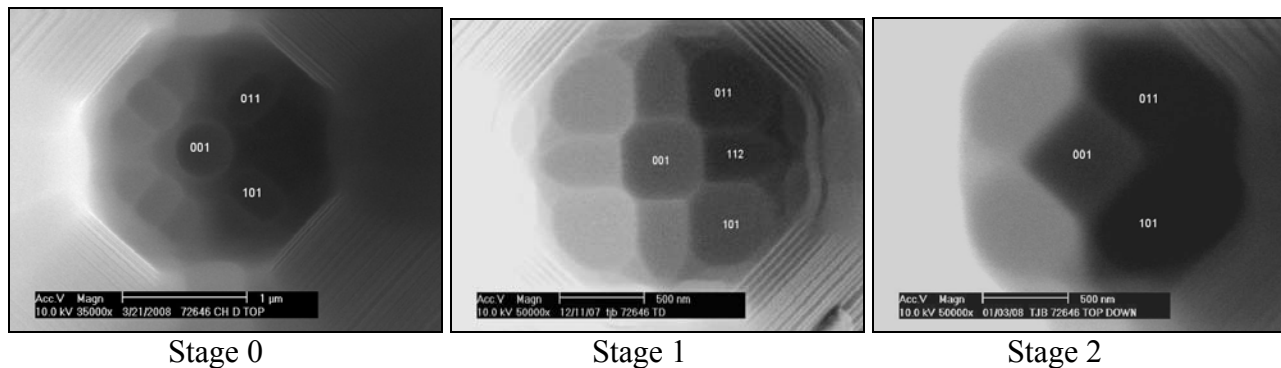


Fig 1 Top down SEM photos show the various end form stages for the ZrO/W(100) Schottky source.

Table I

The β factors and central (100) flat sizes are given for the indicated stage transitions, I' and operating time at 1800 K. This source had an inscribed radius of ~ 750 to 900 nm depending on the end-form stage.

I' (mA/sr)	Time (hrs)	Stage		β (m^{-1})		Flat Size (nm)	
		Initial	Final	Initial	Final	Initial	Final
0.50	93	1	2	1.436×10^5	0.973×10^5	448	490
0.25	29	2	0	0.973×10^5	0.862×10^5	490	452

¹ L.W. Swanson and G. A. Schwind, in Handbook of Charged Particle Optics, Second Edition, edited by J. Orloff (CRC, New York, 2008) Chap. 1, p. 1.

² S. Fujita and H. Shimoyama, Phys. Rev. **B 75**, 2073 (2008).

³ M.S. Bronsgeest and P. Kruit, J. Vac. Sci. Technol. **B 27**(6) 2524 (2009).

⁴ J.P. Barbour, F.M. Charbonnier, W.W. Dolan, W.P. Dyke, E.E. Martin and J.K. Trolan, Phys. Rev. **117**, 1452 (1960).